SLAC-PUB-9499
September 2002

Active and Passive RF Components for High-Power Systems

Sami G. Tantawi and Christopher D. Nantista

Stanford Linear Accelerator Center, 2575 Sand Hill Rd., Menlo Park, CA 94025

Abstract. In recent years, R&D for pulse compression and power distribution systems for the Next Linear Collider has led to the invention of many novel rf components, some of which must handle up to 600 MW of pulsed power at X-band. These include passive waveguide components, active switch designs, and non-reciprocal devices. Among the former is a class of multi-moded, highly efficient rf components based on planar geometries with overmoded rectangular ports. Multi-moding allows us, by means of input phasing, to direct power to different locations through the same waveguide. Planar symmetry allows the height to be increased to improve power handling capacity. Features that invite breakdown, such as coupling slots, irises and H-plane septa, are avoided. This class includes hybrids, directional couplers, an eight-port superhybrid/dual-mode launcher, a mode-selective extractor, mode–preserving bends, a rectangular mode converter, and mode-mixers. We are able to utilize such rectangular waveguide components in systems incorporating low-loss, circular waveguide delay lines by means of specially designed tapers that efficiently transform multiple rectangular waveguide modes into their corresponding circular waveguide modes, specifically TE_{10} and TE_{20} into circular TE_{11} and TE_{01}. These extremely compact tapers can replace well-known mode converters such as the Marié type. Another component, a reflective TE_{01}-TE_{02} mode converter in circular waveguide, allows us to double the delay in reflective or resonant delay lines. Ideas for multi-megawatt active components, such as switches, have also been pursued. Power-handling capacity for these is increased by making them also highly overmoded. We present a design methodology for active rf magnetic components which are suitable for pulse compression systems of future X-band linear colliders. We also present an active switch based on a PIN diode array. This component comprises an array of active elements arranged so that the electric fields are reduced and the power handling capability is increased. Novel designs allow these components to operate in the low-loss circular waveguide TE_{01} mode. We describe the switching elements and circuits.

I. INTRODUCTION

Because of the requirements of the Next Linear Collider high-power rf systems, passive microwave components have developed significantly during the last few years [1,2]. The power handling capabilities of these components have increased considerably [3]. This has been achieved by increasing the size of these components with respect to the operating wavelength, i.e., by overmoding these components. In particular a class of microwave structures that has complete planar symmetry has been developed. These components carry only TE_{n0} modes. This makes it possible to make all the manipulations in the two dimensional plane. The height of these components can then be increased to reduce the field and allow for high power operation. This class of components is overmoded in both height and width. It allows simultaneous

Work supported by the Department of Energy contract DE-AC03-76SF00515.

Invited talk presented at the Fifth Workshop on High Energy Density and High Power RF
October 1-5, 2001, Snowbird, Utah.

manipulation of multiple TE_{n0} modes; i.e. multimoding. Because of this these components can perform several functions at the same time, resulting in compact and efficient system integration. To make a connection between these modes and circular waveguides needed to transfer rf power over long distances, we've developed a special type of multimoded circular-to-rectangular taper. We present the design of these components and show their application to some rf systems.

Another class of multimoded components that depends on the azimuthal symmetry of circular waveguide carrying the TE_{0n} modes has been developed. This class is used to reduce the length of rf storage lines. We present the design methodology and experimental data for this type of component.

We also extend the spirit of overmoded waveguide structures to active and nonreciprocal devices. We present the theory for a nonreciprocal device that operates in the coaxial circular waveguide mode TE_{01}. This device has the potential of handling tens of megawatts at X-band. It could be used as a circulator or as a switch.

Similar attempts have been made to increase the power handling capabilities of bulk effect semiconductor components. Reports have been made on optically controlled semiconductor switches operating in overmoded waveguide [4]. Here we report the development of a switch made from a PIN diode array operating in an overmoded waveguide carrying the TE_{01} mode. The PIN diode rf switch was invented in the middle of the twentieth century [5,6]. PIN diode switches have wide applications at the low to medium power levels. Various packaged PIN diodes are commercially available. However, due to their small size, packaged PIN diodes cannot be used for switching very high power rf signals. At the end of 1960's, a rectangular waveguide switch [7,8] was developed to handle higher power rf signals than packaged PIN diodes. The window switch was tested up to 100 kW at X-band without problem. Thus, the power handling capability of a semiconductor rf switch has been at the level of 100 kW; this is still low for application to active pulse compression systems for future linear colliders.

A high power device can comprise an array of active elements arranged so that the electric fields are reduced and the power handling capability is increased. In this paper, we will discuss high power rf switches, which consist of the active switching elements. The basic idea is to distribute the power into several elements so that the amount of the power to be handled by each element is reduced, in addition to improving the maximum power of each element by designing it in an over moded structure.

II. PLANAR COMPONENTS

The idea for planar components has started by the need for a 3dB hybrid capable of handling hundreds of megawatts of rf power at X-band for a SLED-II pulse compression system [9]. A satisfactory device was designed based on the R.H. Dicke's circuit synthesis of a 3dB hybrid [10] (see Fig. 1). Then it was realized that the two interconnecting guides could be combined into one single guide carrying two modes [11] as shown in Figure 1. This resulted in the so-called magic-H hybrid. The device

has full planar symmetry, and the height can be adjusted to any value required to reduce surface field and increase power handling capacity.

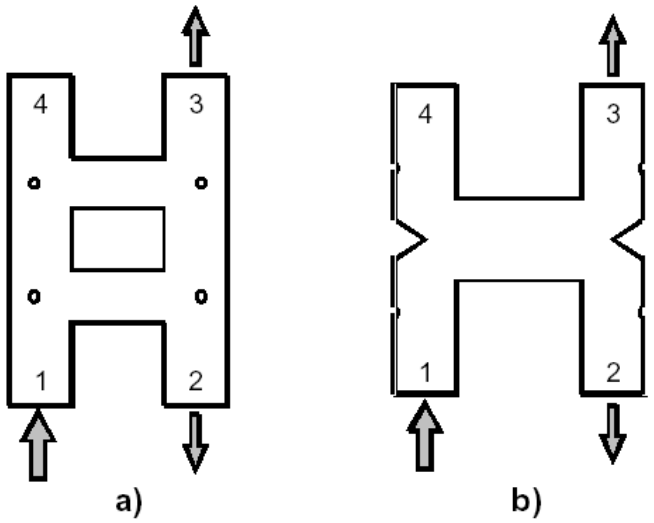

FIGURE 1. Schematic of the h-planar geometries of the a) two-rung ladder and b) "magic H" hybrid designs. Power-flow arrows indicate output ports for the indicated input port.

By putting two of these hybrids together, side-by-side, a dual moded waveguide with similar dimensions as the connecting guide could be produced (see Fig. 2). Adding the remaining parts of the hybrid to this device resulted into the invention of the so-called cross potent superhybrid [12] (see Fig. 2).

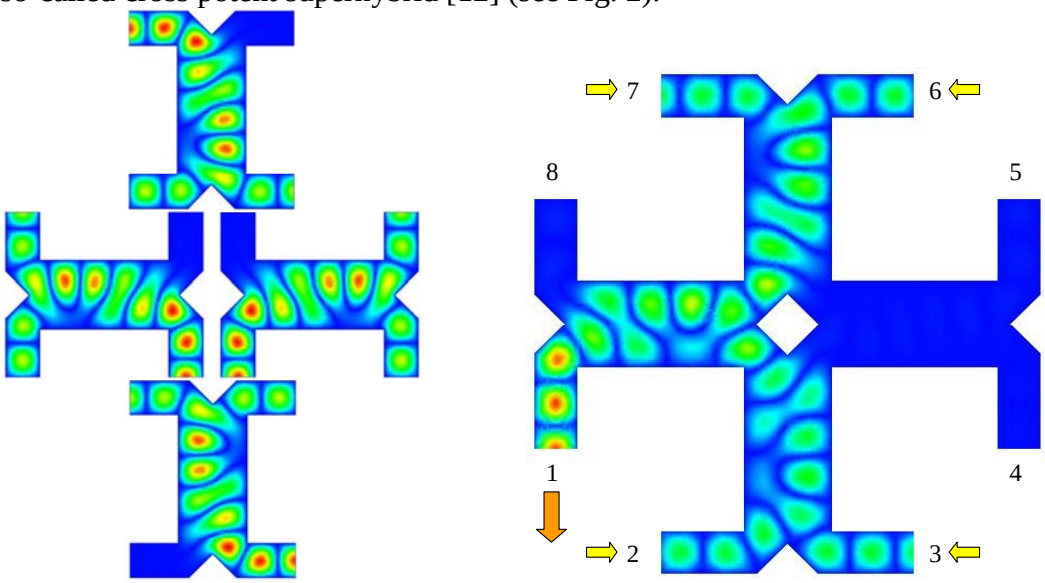

FIGURE 2. Combining four H-plane hybrids resulted in the invention of the Cross Potent Superhybrid

This superhybrid can be used to combine power from four rf sources into any one of four outputs. The choice of the output port depends on the phases of the inputs. The scattering matrix of the device is given by:

$$\mathbf{S}_{cp} = \frac{1}{2}\begin{bmatrix} 0 & 1 & -i & 0 & 0 & -1 & -i & 0 \\ 1 & 0 & 0 & -i & -1 & 0 & 0 & -i \\ -i & 0 & 0 & 1 & -i & 0 & 0 & -1 \\ 0 & -i & 1 & 0 & 0 & -i & -1 & 0 \\ 0 & -1 & -i & 0 & 0 & 1 & -i & 0 \\ -1 & 0 & 0 & -i & 1 & 0 & 0 & -i \\ -i & 0 & 0 & -1 & -i & 0 & 0 & 1 \\ 0 & -i & -1 & 0 & 0 & -i & 1 & 0 \end{bmatrix}$$

One variation on this device is achieved by eliminating two of the output ports in exchange for a single port carrying two modes. Figure 3 shows such a device that can launch either the TE_{10} or the TE_{20} modes in one single port depending on the phases of the input devices. Dealing with two modes at once, TE_{10} and TE_{20}, is possible. For example Figure 4 shows bends that transfer these two modes perfectly at the same time. For the theory for these bends the reader is referred to [13].

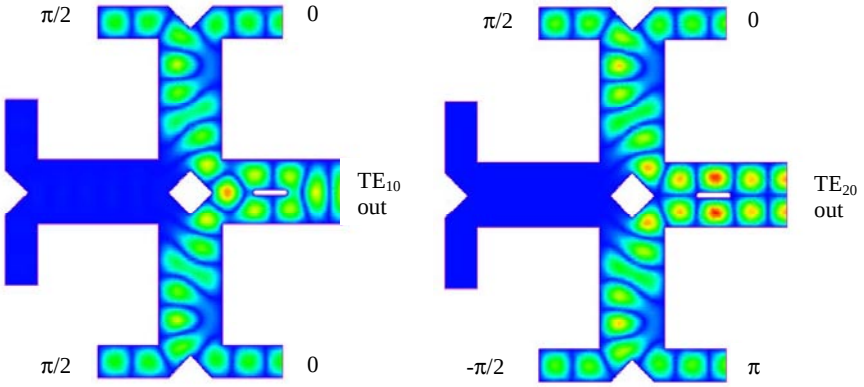

FIGURE 3. Cross Potent Launcher with simulated electric field plots illustrating launching a) TE_{10} and b) TE_{20} in the right overmoded rectangular port with the indicated relative phases for four equal amplitude inputs. Alternate phasings of the inputs send the power to either of the left ports.

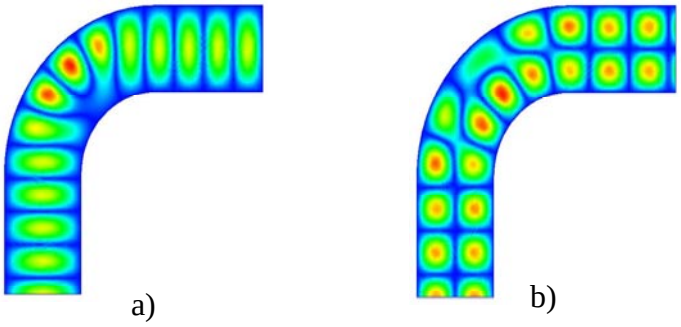

FIGURE 4. Overmoded H-plane bend waveguide with simulated electric field plots illustrating a) TE_{10} mode transmission and b) TE_{20} mode transmission.

One can also mix those two modes by making an H-plane bend in these planar waveguides (see Fig. 5). Using this and the center part of the cross potent superhybrid,

one can make a device that separates these modes into different waveguides (see Fig. 5). Indeed, these designs are not unique. For example, another design that can separate these two modes is shown in Figure 6.

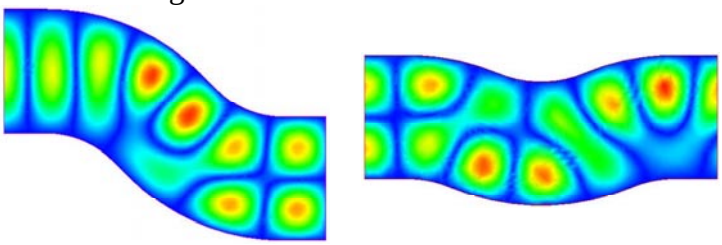

Jog Converter with HFSS simulated electric fields illustrating conversion from TE_{10} to TE_{20} (left to right) or from TE_{20} to TE_{10} (right to left).

Mode Mixer with HFSS simulated electric fields illustrating conversion from TE_{20} to an equal mixture of TE_{10} and TE_{20}.

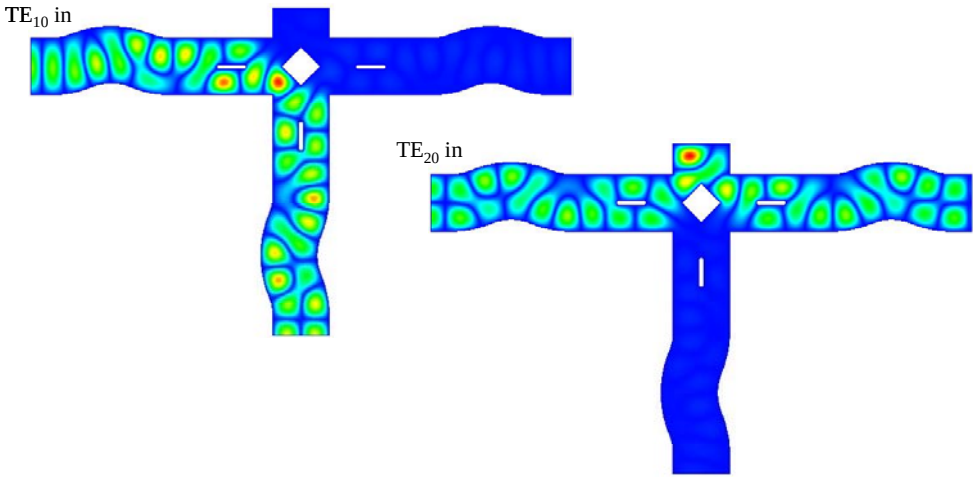

FIGURE 5. Mode mixers and some of their use in mode separators or mode extractors

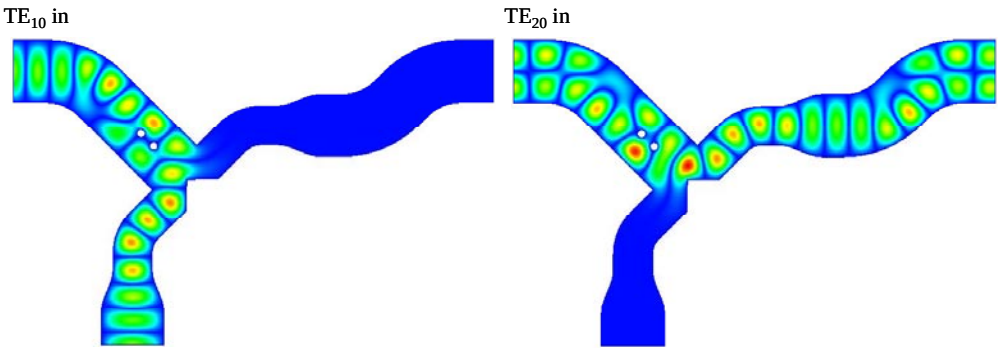

FIGURE 6. Mode-Selective Extractor

To connect these devices with circular waveguides, which is being used for low-loss energy transfer and storage, we use a special type of circular-to-rectangular taper [14]. This taper converts the rectangular guide TE_{10} mode into the TE_{11} mode of

circular guide and the rectangular TE_{20} into the low-loss TE_{01} mode of the circular guide (see Fig. 7).

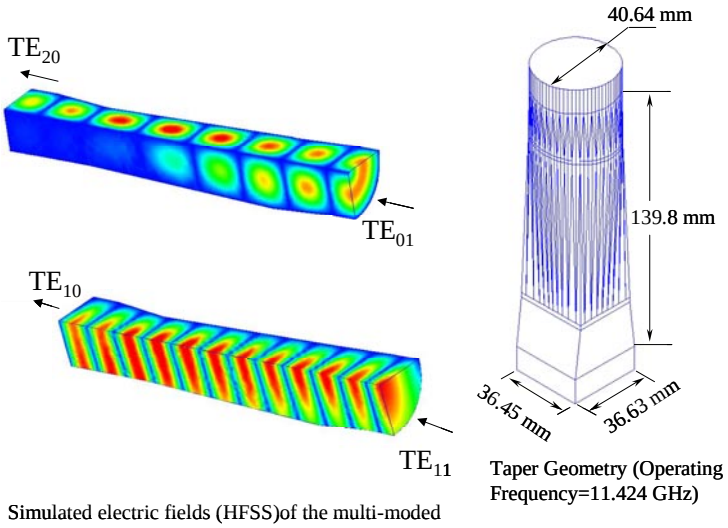

FIGURE 7. Dual-Moded Rectangular/Circular Converter/Taper

Based on these components, it is possible to design several high power rf pulse compression systems. For example, the Delay Line Distribution System (DLDS) [15] could be greatly simplified using these components (see [13]).

III. MULTIMODED DELAY LINES

All pulse compression systems considered for the NLC use very long runs of low loss overmoded circular waveguide [16]. The SLED-II system [9] is of particular interest because it minimizes these runs. Yet, even an rf pulse compression system based on SLED-II may use hundreds of kilometers of waveguide for the full installation.

Here we show a method for reducing these long runs of waveguides by making them multimoded. Consider the delay line shown in Figure 8.

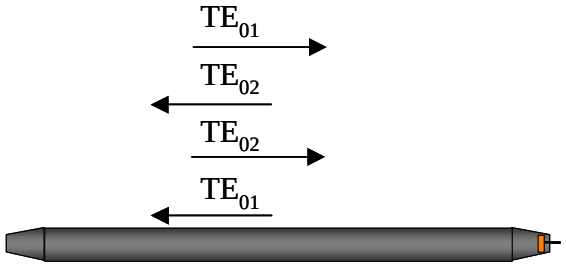

FIGURE 8. Dual-moded delay line

The rf signal is injected into the delay line waveguide in the TE_{01} mode. This is the only azimuthally symmetric TE mode supported at the input port. The waveguide is then tapered up to a diameter that supports several TE_{0n} modes. The TE_{01} mode travels

all the way to the end of the delay line and then gets reflected and converted into the TE_{02} mode. The TE_{02} mode travels back to the beginning of this line and, since the input of the line cuts off this mode, gets reflected. If the input taper is designed carefully, TE_{02} can be reflected perfectly. Then, because of reciprocity, the TE_{02} wave gets converted back to TE_{01} at the end of the line. This mode then travels back and exits the line. The total delay in the delay line is twice that seen by a single moded line. Hence, one can cut the length of delay line by a factor of two.

The End Mode Converter

The mode converter at the end of the delay line is shown in Figure 9. It is basically a step in the circular waveguide. If the big waveguide supports only the TE_{01} and the TE_{02} mode among all TE_{0n} modes and the small waveguide supports only the TE_{01} mode, then the device could be viewed as a three-port network. One can choose the diameter of the small guide such that the couplings between each mode in the large guide and the single mode in the small guide are equal. In this case, it is a symmetrical three-port network. A theory for such a device is presented in [17]. It shows that there exists a position for placing a short circuit in the middle arm of this three-port network (the small guide in this case) that makes it possible to transfer the power perfectly between the remaining two arms, or in this case between the TE_{01} and the TE_{02} modes in the large guide.

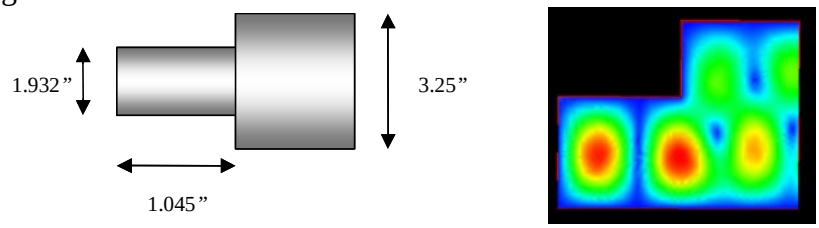

FIGURE 9. TE_{01}-TE_{02} reflective mode converter. The dimensions shown are for an operating frequency of 11.424 GHz. The field pattern shown from finite element simulations predicts a peak electric field of 26.6 MV/m for 300 MW of input power.

The only step left in the design of this end mode converter is a careful taper design that reduces the diameter of the delay line into the diameter of a waveguide that can support only TE_{01} and TE_{02} modes. The taper needs to transfer both modes perfectly.

Experimental Results

Figure 10a shows the delay through a 75 ns delay line with a short circuit at the end for a total delay of 150 ns. Figure 10b shows the delay after placing the mode converter at the end of this line. The delay was doubled at the expense of increased loss. The loss can be brought back down by using larger diameter waveguide for the delay line.

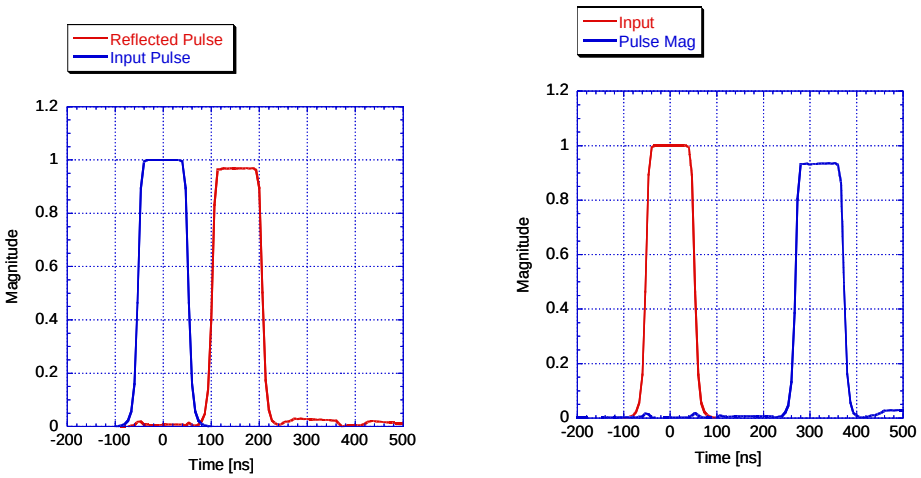

(a) (b)

REPLACE THIS TEXT WITH THE FIGURE GRAPHIC

FIGURE 10. (a) Measured delay through 75 feet of WC475 waveguide terminated with a flat plate. The round trip delay time is 154 ns. (b) Measured delay through 75 feet of WC475 waveguide terminated with the TE_{01}-TE_{02} mode converter. The round trip delay time is 320 ns. The operating frequency is 11.424 GHz.

IV. ACTIVE SEMICONDUCTOR DEVICES

A new active window, PIN/NIP diode array active window, which is operated at TE_{01} mode in the circular waveguide was proposed and developed [18]. Our active window is designed and built to avoid the difficulties of the TE_{10} mode rectangular waveguide window switch and to handle X-band rf signals at multi-megawatt levels. This is achieved by

- using an overmoded structure, thus increasing the cross sectional area and reducing the power density.
- using the TE_{01} mode in circular waveguide, which has no electric field at the waveguide wall, thus avoiding edge effects, for a more robust design.

In this section, we describe the design of our PIN/NIP diode array active window.

The Silicon Window

The conceptual view of our active window is illustrated in Figure 11. The base material of the window is highly pure silicon. This window is located in a circular waveguide, which is operated at the TE_{01} mode. As shown in the figure, the PIN/NIP diode structure is a set of radial lines. Each line is heavily doped by P-type and N-type impurities on the topside and backside surfaces, respectively. Each diode line is covered by a metal line, which supplies bias voltage and current to the diode line. The TE_{01} electric field orientation is also indicated in Figure 11. All electric field lines are in the azimuthal direction; i.e. the diode lines are perpendicular to the electric field of the rf signal. This means that the reflection caused by the diode structure and the metal

lines is very small when the active window is reverse or zero biased; the rf signal only sees the dielectric contribution of the bulk silicon material. This is the *off* status of the active window. To minimize the reflection from the lines, the *coverage factor*, which is defined as the ratio of the area of the diode structure to that of the whole active region of the window, is chosen to be 10%. The P lines on the front and the N lines on the back are arranged to alternate with each other (see Figure 11). A side-cut view of the active window illustrates the idea (see Figure 12). When forward bias is applied, a massive number of injected carriers goes across the I region. Since the P and N lines are alternating, the injected carriers fill the I region, and the incident rf signal is reflected. This is the *on* status of the active window. The thickness of the active window, which is the same as the I region width in this design, must be small enough so that the carriers injected from the heavily doped P and N lines by the forward bias can diffuse through the high receptivity I region to the heavily doped lines on the other side. This is a very important point to achieve good rf isolation at the *on* status. The carrier lifetime in the high resistivity silicon material is closely related to the diffusion length of the carriers. It is given by $L_D = (\tau D_{AP})^{1/2}$, where L_D is the diffusion length of the carriers, τ is the carrier lifetime in the silicon material, and D_{AP} is the diffusion coefficient. The diffusion coefficient in silicon is D_{AP} = 15.6 cm^2/s, giving $L_D \approx 40(\tau(\mu\,\mathrm{sec}))^{1/2}\,\mu m$. Hence, the base material of the active window must be very pure silicon and must have long carrier lifetime to achieve good conductivity modulation with forward bias. While this puts an upper limit on the window thickness, there is a lower limit for this thickness. If the window is much thinner than the skin depth, good isolation of the rf signal would not be obtained. If we assume the carrier density to be $10^{17} cm^{-3}$ in the I region with forward bias, then the skin depth δ_s can be calculated with knowledge of the carrier motility in silicon. At a frequency of 11.424 GHz, $\delta_s \approx 100$ µm.

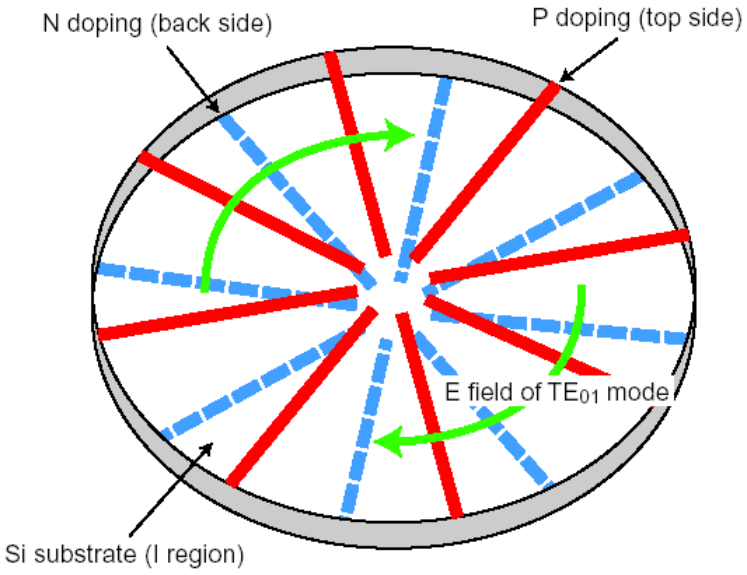

FIGURE 11. Conceptual view of PIN/NIP diode active window.

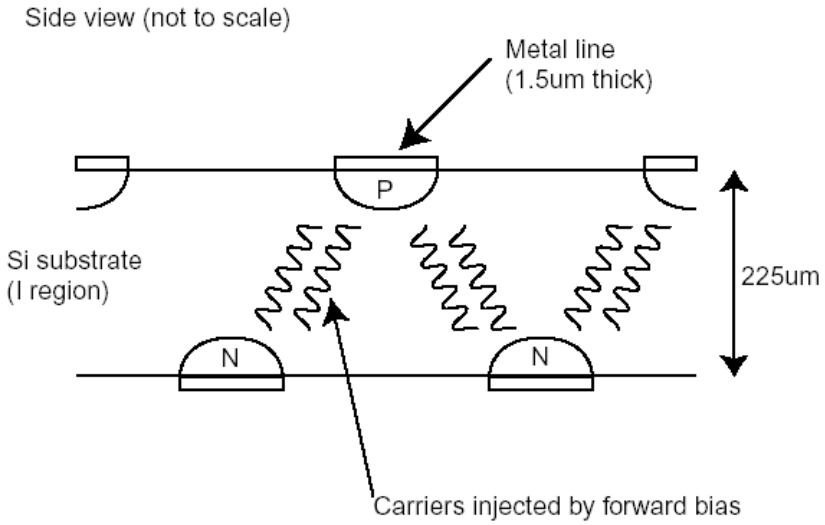

FIGURE 12. Side view of PIN/NIP diode active window.

In the actual design of our prototype active window, the diode structure consists of 400 radial lines each on the front and back. The width of the radial lines is tapered from 25 μm near the waveguide surface to 2 μm near center of the window. The line width and the number of lines are chosen so that the coverage factor is 10%. The thickness of the window is 225 μm. If the carrier density achieved 10^{17}cm^{-3}, this thickness is more than the skin depth of the intrinsic region for X-band rf signals.

At this carrier density, the surface resistance $R_s \approx 4.8$ ohms at our operating frequency of 11.424 GHz. The diameter of active region and waveguide is 1.299 inches, so that the waveguide impedance is 4.16 times the impedance of vacuum. Hence, the loss dissipated in the window when the window is *on* is given by

$$L_0 \equiv P_l(total)/P_{in} = 4\frac{R_s}{Z_g} \approx 1.23\% .$$

RF Structure and Window Support

The rf structure to support the window is shown in Figure 13. It consists of two aluminum circular waveguides with steps, a ceramic ring, and metal springs. The active window is located between the two waveguides. The ceramic ring fixes the active window at the design position.

The TE_{01} mode rf signal is launched by a compact wrap-around mode converter (see [3]). The diameter of the waveguides changes from 1.5 inches to 1.3 inches at the center by steps designed so that the whole rf structure is matched *without* the window. Since silicon has a large dielectric constant, the impedance mismatch at the surface of the active window is large, causing non-negligible reflection. Because we are interested in the pure characteristics of the active window, the structure was designed without matching sections to compensate for the mismatch at the window surfaces.

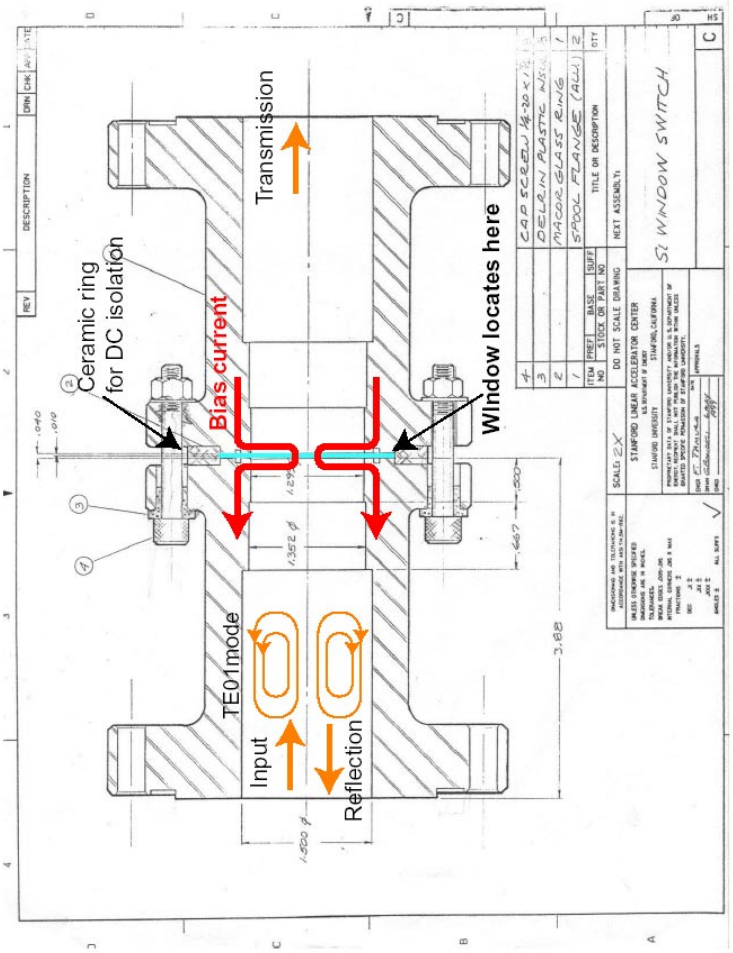

FIGURE 13. Active window and rf structure.

The two waveguides are DC separated. The ceramic ring works as the DC voltage gap. There are metal springs between the active window and the waveguides. The waveguides are connected to a biasing circuit. The biasing voltage is supplied to the active window through the waveguides and the springs, and the waveguides are DC isolated from the TE_{01} mode converters by mylar insulators.

There is a gap between the two waveguides, but no choke structure. Since the surface currents of TE_{01} mode in circular waveguides are azimuthal, the gap does not cut any surface currents and there is no rf leakage through the gap. Indeed, this a big advantage of this structure over TE_{10} mode rectangular window switches; we can avoid the complex choke geometry necessary in the rf structures of this later type.

Finally, vacuum seals necessary for high power operation under vacuum are made with Viton rubber gaskets for DC isolation.

Experimental Results

The high power experiment was performed with an X-band klystron (XL-2) and a SLED-II rf pulse compression system at SLAC. A high power rf signal of 900 ns pulse

duration at 11.424 GHz was generated by the klystron, compressed by the SLED-II system, and fed to the active waveguide window. The SLED-II system allowed us to operate the klystron at a relatively low power level and acted as a buffer between the klystron and the unmatched window. The power level output to the active window was up to 15 MW. For our experiments, this was high enough. The compressed rf pulse duration was 150ns. The repetition rate was limited to 5 Hz, since the active window did not have cooling.

The incident, reflected, and transmitted rf signals were measured by power meters and rf diode detectors through directional couplers. The TE_{01} mode converters have view-ports to watch the surfaces of the window so that the video camera could detect flashes of light if arcs occur on the surface of the active window.

Two types of silicon windows were prepared for this high power experiment. First one is an active window, which has a full PIN/NIP diode array structure on both the front and back. This active window is the 10^{17} cm^{-3} doping density version. The resistivity of the base material is 5000 ohm-cm. The window thickness is 225 μm. The second one had only the metal line structure on one side and no doping line structure; the other side had no structure (*metal-only version*). This version of the window was prepared for investigating the breakdown properties of the thin metal structure. The resistivity of its base material is 1000 ohm-cm and its thickness is 315 μm.

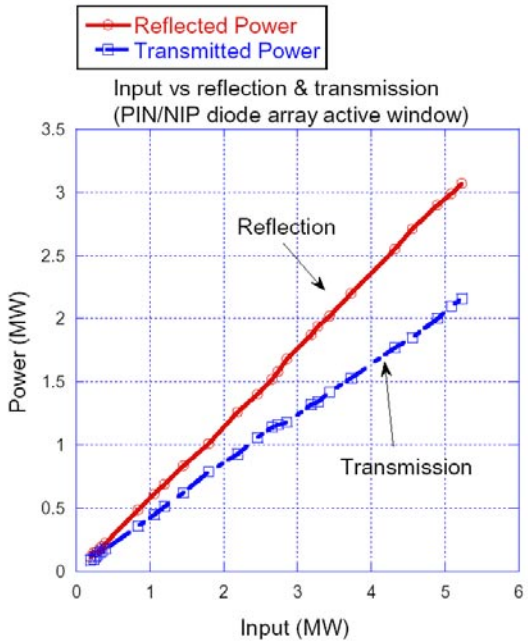

FIGURE 14. Input versus transmission and reflection power.

In Figure 14, the reflected and transmitted powers from the active window with full diode structure are plotted. As shown in the figure, the reflected and transmitted powers were proportional to the input power. Hence, the reflection coefficient did not change and the loss dissipated into the active window did not increase with increasing the input power up to 5.2MW. This means that avalanche breakdowns did not occur at

this power level. If the avalanche breakdown occurred, there would be copious carriers in the intrinsic region, and the reflection coefficient would have changed.

However, arcing started at an input power level of around 4 MW. When arcing occurred, the vacuum in the system went from 10^{-8} Torr at normal operation to above 10^{-5} Torr, and interlocks stopped the klystron. After the onset of arcing, the reflected power increased and the transmitted power slowly decreased.

This arcing was very vacuum dependent. We had to process slowly from the lower power levels after the trips. Flashing lights were observed by the video camera from both sides when the arcing occurred. These characteristics, vacuum dependency and flashing lights, are typical characteristics of the vacuum breakdowns, not of avalanche breakdowns.

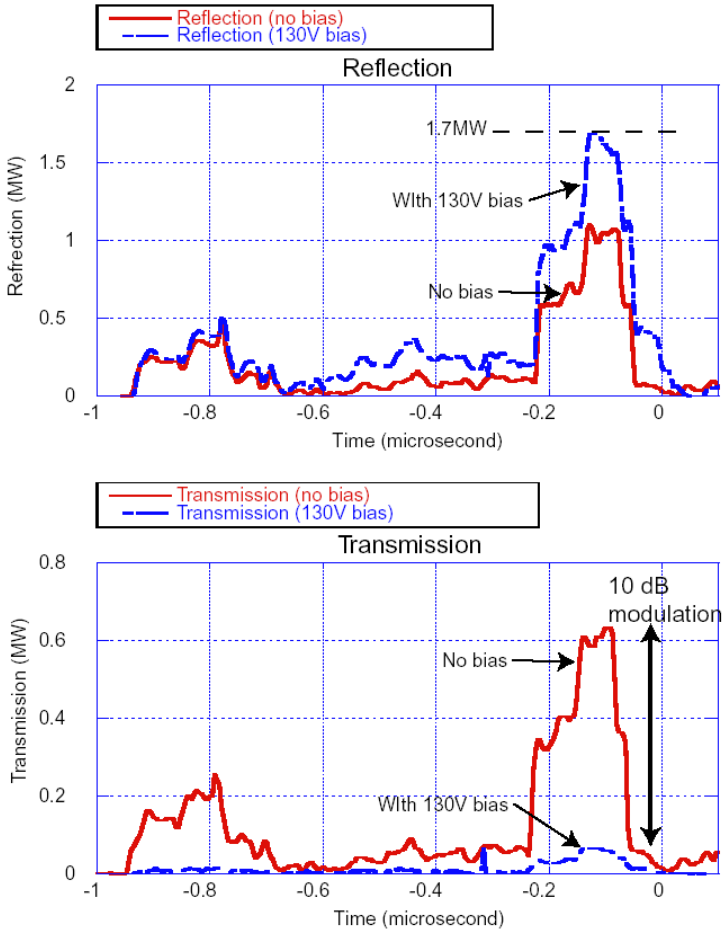

FIGURE 15.Waveform with zero bias and 130V forward bias.

After achieving the maximum input power of 5.2 MW, the arcing occurred more and more frequently, and also at lower power levels. We could not raise the input power further. Thus, the high power operation was limited by arcing. The maximum field at the surface of the window is calculated as 3.8 MV/m at 5.2 MW.

The waveforms of the transmitted and reflected rf signal with and without the forward bias voltage are shown in Figure 15. With the forward bias voltage at 130 volts, the reflection increased and the transmission decreased. The reflected rf signal was modulated from 1.1 MW to 1.68 MW, and the transmitted rf signal was modulated from 0.63 MW to 60 kW. A 10 dB of transmission modulation was thus achieved. With the forward bias, no arcing on the surface of the active window was observed, which is reasonable because the active window is a conductor, and the electric field of rf signal is minimum near the window surface.

V. ACTIVE MAGNETIC DEVICES

The implementation of a circulator or a switch can be achieved using a two-port nonreciprocal network plus a 3dB hybrid and a splitter (see Fig. 16). The simplest implementation of the nonreciprocal element in an overmoded waveguide using the TE_{01} mode is shown in Figure 17. This implementation also depends on the so-called wrap-around mode converter [3]. In this system the mode converter launches the TE_{01} mode, which has both axial and radial magnetic fields, in a coaxial structure. At the ends of the structure, the coaxial guide becomes narrow and only the coaxial TEM mode can propagate (see Fig. 2). A pulsed current signal could be launched from that narrow port (port-A in Fig. 2) This pulse would have only azimuthal magnetice field. This field is used to bias a piece of garnet wrapped around the center conductor of the coaxial structure. This structure has several advantges for handling high power rf signals:

1- Operating in an overmoded waveguide, with a large cross sectional area for a given wavelength, should give the device a high power handling capacity.
2- All rf electric field lines are parallel to the interface between the garnet material and vacuum (see the theory section below).
3- The center conductor could be used to cool the garnet material; it could be made as a tube with water flowing through the center.

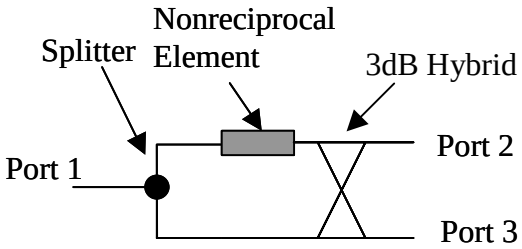

FIGURE 16. This three-port network will work as a circulator if the phase shift through the two-port nonreciprocal element differs by 180 degrees for different propagation direction. The system could work as a switch if one can control the phase shift through the element.

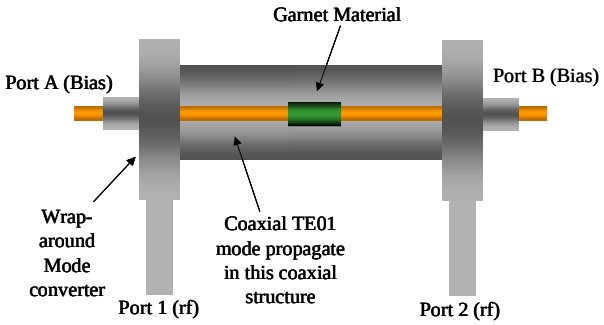

FIGURE 17. Nonreciprocal two-port device employing the TE_{01} mode.

Several variations on this device are possible. An elegant implementation of the system shown schematically in Figure 16 is illustrated in Figure 18. In this geometry the splitter is realized by dividing the power between the TE_{01} and the TE_{02} modes. These two modes interact with the garnet coated section in different manners. To implement the circulator, one could design the system to make the phase difference between these two modes in the forward direction differ from that of the backward direction by π. To implement a switch, one could control that phase difference by varying the current in the center conductor.

For a proof of principle numerical experiment we considered the properties of calcium vanadium doped garnet [19]. We chose this material because of its narrow line width. The calculated values for μ and k of its permeability tensor are shown in Figures 5 and 6. The operating frequency used to generate these curves is 11.424 GHz. The dielectric constant of this material is about 14. The biasing magnetic field was chosen so that the material would operate below the resonance frequency.

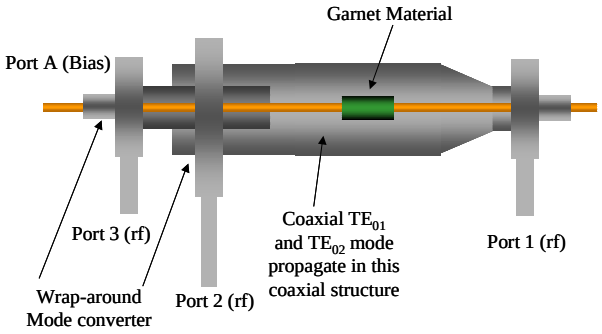

FIGURE 18. Implementation of the overmoded circulator/switch.

Figure 19 shows the required garnet thickness and length for a π phase difference between forward and backward TE_{01} mode waves. For the optimum thickness, the rf losses are less than one percent. This is a manageable loss level whose heat can be removed by cooling through the center conductor.

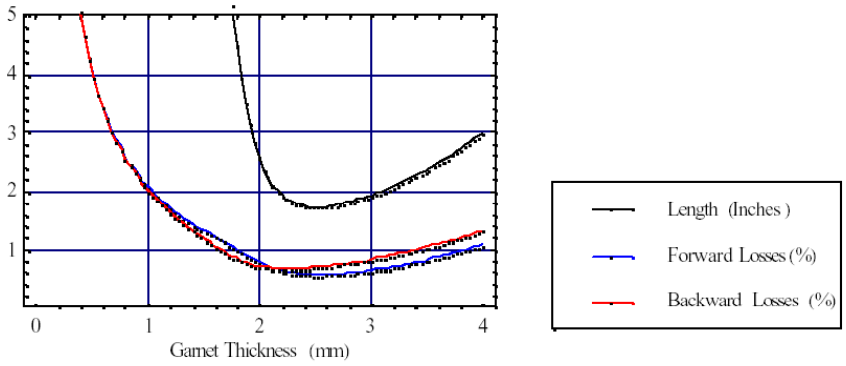

FIGURE 19. The required dimensions of the garnet material for a π phase shift between forward and backward waves for the TE_{01}.

VI. CONCLUSIONS

In this paper, we have presented an overview of some developments made over the past few years in the area of high power microwave components. This work has been motivated by the requirements of an rf system for a next generation electron-positron linear collider, which must handle X-band power levels up to hundreds of megawatts. These components are thus all overmoded to ameliorate breakdown problems associated with high fields.

They include several passive waveguide devices that make use of multi-moding for directing power through phasing of combined sources. These take advantage of planar symmetry for ease of mode manipulation and height-independence of the designs. They also include mode converters between rectangular waveguide modes, between rectangular and circular waveguide modes, and between circular waveguide modes. The latter device can be used to double the storage time in a reflective delay line.

Some novel active components, activated by pulsed voltage or current, have also been described. These include a PIN diode array on a silicon wafer operating as an rf window and a garnet based nonreciprocal waveguide structure. Some experimental results for the former at multi-megawatt operation have been presented. Both take advantage of the TE_{01} mode field pattern in circular waveguide. Either of these devices, although they require further development, have the potential of providing the basis for a high power microwave switch.

ACKNOWLEDGMENTS

The authors would like to thank Professors Ronald Ruth, Perry Wilson, Norman Kroll and Roger Miller for many useful discussions. We would like to thank Gordon Bowden for his help in constructing the rf structure. The semiconductor switch work was done in collaboration with Fumihiko Tamura. We are also grateful for the help and effort of Chuck Yoneda and the vacuum group at the Klystron Department at SLAC.

This work was supported the US Department of Energy contract DEAC03-76SF00515.

REFERENCES

1. Sami G. Tantawi, “New Development in RF Pulse Compression,” Proc. of the XX International Linac Conference, Monterey, California, USA, August 21 - 25, 2000, p. 673-677, and the references cited therein.
2. Christopher D. Nantista and Sami G. Tantawi, "A Planar Rectangular Waveguide Launcher and Extractor for a Dual-Moded RF Power Distribution System," Proc. of the XX International Linac Conference, Monterey, California, USA, August 21 - 25, 2000.
3. S.G. Tantawi, *et al.*, "The Generation of 400-MW RF Pulses at X Band Using Resonant Delay Lines," *IEEE Trans. Microwave Theory Tech.*, vol. 47, no. 12, pp. 2539-2546, Dec. 1999; SLAC-PUB-8074.
4. Sami G. Tantawi, Ronald D. Ruth, Arnold E. Vlieks, and Max Zolotorev, “Active high-power RF pulse compression using optically switched resonant delay lines,” IEEE Transactions on Microwave Theory and Techniques, MTT-45(8), August 1997, p. 1486–1492.
5. S. M. Sze, “Physics of Semiconductor Devices,” John Wiley & Sons, second edition, 1981.
6. Joseph F. White, “Microwave Semiconductor Engineering,” Van Nostrand Reinhold Company, New York, 1982.
7. Kenneth E. Mortenson, Jose M. Borrego, Paul Bakeman, E. Jr., and Ronald J. Gutmann, “Microwave silicon windows for high-power broad-band switching applications,” IEEE Journal of Solid-State Circuits, SC-4(6), December 1969, p. 413–421.
8. Kenneth E. Mortenson, Albert L. Armstrong, Jose M. Borrego, and Joseph F. White, “A Review of Bulk Semiconductor Microwave Control Components,” Proceedings of the IEEE, 59(8), August 1971, p. 1191–1200.
9. P. B. Wilson, Z. D. Farkas, and R. D. Ruth, "SLED II: A New Method of RF Pulse Compression," Linear Accl. Conf., Albuquerque, NM, September 1990; SLAC-PUB-5330.
10. Montgomery, Dicke, and Purcell, Principles of Microwave Circuits, Rad. Lab. Series, 1948, p. 451.
11. C.D. Nantista, W.R. Fowkes, N.M. Kroll, and S.G. Tantawi, “Planar Waveguide Hybrids for Very High Power RF,” proc. Of the 1999 IEEE Particle Accelerator Conference, New York, N.Y., March 29-April 2, 1999.
12. Christopher D. Nantista and Sami G. Tantawi, "A Compact, Planar, Eight-Port Waveguide Power Divider/Combiner: The Cross Potent Superhybrid," IEEE Microwave Guided Wave Lett., vol. 10, no. 12, pp. 520-522, December 2000; SLAC-PUB-8771.
13. Christopher D. Nantista and Sami G. Tantawi, "Multi-Moded Passive RF Pulse Compression Development at SLAC," proc. of Advanced Accelerator Concepts Workshop, Santa Fe, NM, June 10-16, 2000.
14. S.G. Tantawi, N.M. Kroll, and K. Fant, “RF Components Using Over-moded Rectangular Waveguides for the Next Linear Collider Multi-Moded Delay Line RF Distribution System,” Proc. Of The IEEE Particle Accelerator Conference, New York City, March 29th - April 2nd, 1999, p. 1435-1437.
15. H. Mizuno, Y. Otake, “A New Rf Power Distribution System For X Band Linac Equivalent To An Rf Pulse Compression Scheme Of Factor 2**N,” 17th International Linac Conference (LINAC94), Tsukuba, Japan, Aug 21 - 26, 1994.
16. S.G. Tantawi, R.D. Ruth, and P.B. Wilson, “A Comparison Between Pulse Compression Options for NLC,” proc. of IEEE Particle Accelerator Conference (PAC 99), New York, 29 Mar - 2 Apr 1999. Published in *New York 1999, Particle accelerator, vol. 1* 423-425.
17. Sami G. Tantawi and Mikhail I. Petelin, “The Design and Analysis of Multi-Megawatt Distributed Single Pole Double Throw (SPDT) Microwave Switches,” in IEEE MTT-S Digest, 1998, pp. 1153–1156.
18. Fumihiko Tamura and Sami G. Tantawi, “Development of High Power X-band Semiconductor RF Switches for Pulse Compression Systems of Future Linear Colliders,” proceedings of the XX International Linac Conference, Monterey, California, USA, August 21 - 25, 2000.
19. http://www.trans-techinc.com/catalog/pdfs/pg1-4&5.pdf